SPANDIDOS PUBLICATIONS

Overexpression of human selenoprotein M differentially regulates the concentrations of antioxidants and H_2O_2, the activity of antioxidant enzymes, and the composition of white blood cells in a transgenic rat

DAE YOUN HWANG, JI SOON SIN, MIN SUN KIM, SU YOUN YIM, YONG KYU KIM, CHUEL KYU KIM, BYOUNG GUK KIM, SUN BO SHIM, SEUNG WAN JEE, SU HAE LEE, CHANG JOON BAE, BYOUNG CHUN LEE, MEE KYUNG JANG, JUNG SIK CHO and KAB RYONG CHAE

Laboratory Animal Resources Team, National Institute of Toxicological Research, Korea FDA, Seoul 122-704, Korea

Received September 11, 2007; Accepted October 25, 2007

Abstract. Selenoprotein is associated with a variety of serious diseases, including infectious diseases, neurodegenerative disorders, cancer and cardiovascular disease. The aim of this study was to produce a new transgenic (Tg) rat expressing human selenoprotein M (SelM) in order to examine the protective function of the antioxidant status *in vivo*. To achieve this, a new lineage of Tg rats was produced by the micro-injection of *pCMV/GFP-hSelM* constructs into a fertilized rat egg. Several conclusions can be drawn based on the results of the present study. The human SelM gene was successfully expressed at both the transcription and protein levels in the CMV/GFP-hSelM Tg rats. This Tg rat showed a different enzyme activity for the antioxidant protein in the various tissues examined. In response to the 2,2'-azobiz(2-amidino-propane) dihydrochloride (AAPH) injection, the Tg rats showed a lower level of antioxidant and H_2O_2 concentration as the activity of the antioxidant enzyme was maintained at a higher level in the Tg rats than in the non-Tg rats. Also, the neutrophil-to-lymphocyte ratio was significantly increased in this Tg rat, even though the level of corticosterone remained unchanged in both genotypes. Thus, the results of this study demonstrated that the CMV/GFP-hSelM Tg rat can serve as an animal model for the maintenance of a high level of antioxidant status and can be used to study the biological function of selenoprotein in infectious diseases, cardiovascular disease and cancer.

Correspondence to: Dr Dae Youn Hwang, Laboratory Animal Resources Team, National Institute of Toxicological Research, Korean FDA, 5 Nokbun-dong, Eunpyung-ku, Seoul 122-704, Korea
E-mail: dyhwang@kfda.go.kr

Key words: selenoprotein M, transgenic rat, 2,2'-azobiz(2-amidinopropane) dihydrochloride, superoxide dismutase, glutathione peroxidase

Introduction

Selenoproteins are enzymes that contain selenium in the form of selenocystein in their catalytic center. Until recently, there were 25 known genes encoding selenoproteins in the sequenced human genome (1). However, by means of the 75Se pulse labeling of rats and 2D gel electrophoresis, more than 30 selenoproteins have been detected in various tissues (2). Furthermore, several studies reported that these proteins were tightly associated with a variety of chronic diseases. Glutathione peroxidase (GPX), thioredoxin reductase, methionine-sulfoxide-reductase and SelP are serious infection-related selenoproteins involved in antioxidant defense and intracellular redox regulation and modulation (3,4). Several selenoprotein activities have also been detected in the human and rodent brain. These activities were significantly altered in a number of neurological disorders, including epilepsy, Parkinson's disease, and Alzheimer's disease (3,5). In particular, considerable data from animals and humans have indicated that selenoprotein is effective in reducing the incidence of several different types of cancer, including cancers of the prostate and breast (6).

SelM was first reported as a 0.7-kb cDNA gene that encoded a new selenoprotein identified from the mammalian EST database. This gene has a 145-amino acid open reading frame beginning with an ATG codon in favorable Kozak context and contains an in-frame TGA as the Sec codon. Furthermore, homologous proteins were found in the rat, zebra fish, and other vertebrates, and Sec was conserved in these homologs (7). All previously characterized eukaryotic selenoprotein genes contain a conserved version of the Sec insertion sequence (SECIS) element in the 3' UTR. However, a canonical SECIS element has not been identified in human, mouse, or rat SelM mRNA. In the core motif (AATG A_AA_GA) of the mammalian SelM SECIS element, the AA sequences are replaced with CC sequences. Moreover, a similar computational screen that uses the AATGA_CC_GA pattern detected a novel selenoprotein (SelO) (8). Until recently, there have been few reports on the functional study of SelM. M. Muller *et al* (9) showed that this protein plays a

major role in spicule formation in the demosponge *Suberites domuncula*. In addition, Hwang *et al* (10) suggested that SelM might play a suppressive or protective role in the pathology of patients with Alzheimer's disease. However, no transgenic rat expressing human SelM under the control of the human cytomegalovirus (CMV) immediate early promoter has been available for use in the study of the function of SelM *in vivo*.

In the present study, a novel transgenic rat expressing human SelM (hSelM), which induces the activation of antioxidant protection, was developed. Also, these transgenic rats were shown to have antioxidant protection phenotypes, such as a decrease in total antioxidants and H_2O_2 and an increase in the activity of superoxide dismutase (SOD) and glutathione peroxidase (GPX). These results suggest that the hSelM transgenic rat may be useful for studying the relationship between the antioxidant condition and disease, where a higher level of antioxidant condition exists in specific tissues.

Materials and methods

Plasmid construction. In order to overexpress the hSelM protein, hSelM cDNA was amplified by PCR using the cDNA from the total RNA of the human SK-N-MC neuroblastoma cell line. This reaction was achieved using specific primers (sense, 5'-ATG AGC CTC CTG TTG CCT CCG CTG-3'; antisense, 5'-AGC TGG GGA AGG AAG AAA GTG G-3'), which corresponded to nucleotides 90-113 and 675-696 of the hSclM gene. PCR was carried out using 30 cycles of the following program: denaturation at 95˚C for 30 sec, annealing at 62˚C for 30 sec, and extension at 72˚C for 45 sec. The 606-bp products of the amplified SelM sequence were cloned into the *pGEM-T* vector (A3600; Promega). The SelM fragment (606-bp) was obtained by digesting *pGEM-T-hSelM* with *Sal*I enzymes and cloning them into the *Sal*I site of *pEGFP C-1* (*pCMV/EGFP-hSelM*) (Fig. 1A). The presence and orientation of the hSelM cDNA in the resulting plasmid, named *pCMV/EGFP-hSelM* (6,306-bp), was verified by an automatic sequencer (ABI 373; Perkin Elmer).

Transgenic rat production. The *pCMV/EGFP-hSelM* plasmid was digested with *Stu*I/*Ase*I in order to remove the prokaryotic sequence and then electrophoresed in an agarose gel. The linear gene fragment of the *CMV/EGFP-hSelM* fragment (3,183-bp) was excised and extracted from the agarose gel. The *CMV/EGFP-hSelM* fragment was purified by electropurification, diluted to 4 ng/μl and microinjected into the male pronucleus of fertilized embryos that were obtained by crossing a female with a male Wistar-Imamichi rat. The injected egg was then transferred to the oviducts of a female Sprague Dawley (SD) rat as a pseudopregnant recipient.

Maintenance of the rats and AAPH treatment. Adult Wistar-Imamichi rats were purchased from SJC Inc. in Japan, and the SD rats, as the embryo recipients, were supplied from the breeding center at our institute. All of the rats were kept in an accredited Korean FDA animal facility in accordance with the AAALAC International Animal Care Policies (Accredited Unit, Korea Food and Drug Administration: Unit no. 000996). The rats were given a standard irradiated chow diet (Purina Mills Inc.) *ad libitum* and were maintained in a specified pathogen-free state under a strict light cycle (light on at 06:00 h and off at 18:00 h). All pedigrees were hemizygous for their transgene.

The compound 2,2'-azobiz(2-amidinopropane) dihydrochloride (AAPH) was obtained from Wako Pure Chemical Industrial Ltd. (017-11062; Japan) and dissolved in 1X PBS in order to obtain a final concentration of 135 mg/ml. At 10 weeks of age, the CMV/GFP-hSelM Tg and non-Tg rats were randomly divided into two subgroups (n=6) per group. The first subgroup of Tg and non-Tg rats received a comparable volume of daily 1X PBS via intraperitoneal injections (i.p.) (no-treated Tg and non-Tg group), while the second subgroup received 100 mg/kg body weight (BW)/day of AAPH via i.p. injections (AAPH-treated Tg and non-Tg group). At 5 h after AAPH injection, all of the animals were immediately sacrificed using CO_2 gas in order to prepare the blood and tissue samples, which were then stored in Eppendorf tubes at -70˚C until being assayed.

PCR analysis. The transgene was identified by PCR analysis of the genomic DNA that had been isolated from the tails of the 4-week-old founder rats. This transgene DNA was synthesized using the sense primer 5'-ATG AGC CTC CTG TTG CCT CCG CTG-3' and the antisense primer 5'-AGC TGG GGA AGG AAG AAA GTG G-3', with a complementary *hSelM* cDNA ranging from 90 to 113 and 675 to 696 nucleotides as the DNA template. After 25 cycles of amplification, the level of the *hSelM* product (606-bp) was quantified using the Kodak Electrophoresis Documentation and Analysis System 120 on 1% agarose gels.

For RT-PCR analysis, each tissue sample was frozen in liquid nitrogen. The frozen tissues were chopped with scissors and homogenized in an RNAzol B solution (CS104; Tet-Test Inc.). The concentration of isolated RNA was then determined by UV-spectroscopy. The expression of the transgenes was examined using RT-PCR with 5 μg of the total RNA from each tissue. A total of 500 ng of the oligo-dT primer (18418-012; Gibco BRL) was annealed at 70˚C for 10 min. The complementary DNA, which served as the template for further amplification, was synthesized by adding dATP, dCTP, dGTP and dTTP with 200 units of reverse transcriptase. Ten pmole of the sense and antisense primers were then added, and the reaction mixture was subjected to 28 cycles of amplification. Amplification was carried out in a Perkin Elmer Thermal Cycler using the following cycles: 30 sec at 94˚C, 30 sec at 62˚C and 45 sec at 72˚C. In each case, the minus-RT controls were included in order to differentiate between the DNA and RNA products. RT-PCR was also performed using the primers specific to ß-actin in order to ensure the integrity of the RNA. The primer sequences used for the identification of hSelM gene expression were: sense, 5'-ATG AGC CTC CTG TTG CCT CCG CTG-3'; and antisense, 5'-AGC TGG GGA AGG AAG AAA GTG G-3'. In addition, the primer sequences used to identify rat SelM gene expression were: sense, 5'-CGG ATT GGA CCG TCT TCG A-3'; and antisense, 5'-CCC TCA GCA AGA GTT TAT GC-3'. The sequences of the ß-actin primers were: sense, 5'-TGGAA TCCTG TGGCA TCCAT GAAAC-3'; and

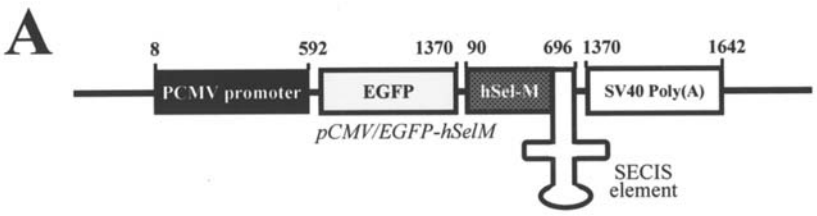

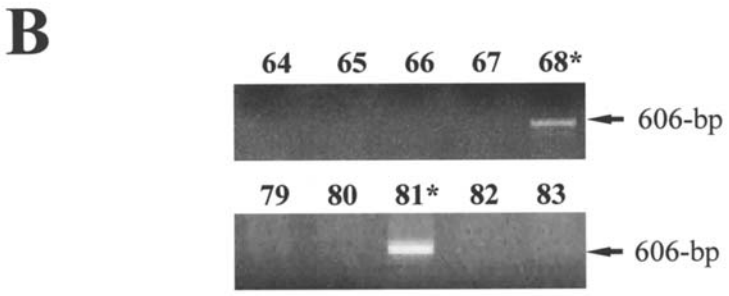

C

Injected Egg	Transfered Egg	Founder rat	Transgenic rat	Efficiency
99	87	28	2	7.1%
		♂ (11) ♀ (17)	♂ (0) ♀ (2)	

Figure 1. The construction of the *pCMV/GFP-hSelM* expression vector and identification of the Tg using PCR. (A) pCMV/GFP-hSelM transgene was constructed based on the GFP expression system, which is a GFP fusion protein under the control of the CMV promoter. hSelM cDNA containing the SECIS element was amplified from RT-PCR using specific primers and was cloned into the *pCMV/GFP/SV40* vector under the control of the CMV promoter. (B) DNA-PCR was performed on the genomic DNA isolated from the tail of a founder rat, and the resulting products (606-bp) are shown. (C) Efficiency of the transgenic rat production.

antisense, 5'-TAAAA CGCAG CTCAG TAACA GTCCG-3'. The experiment was repeated three times, and all samples were analyzed in triplicate.

Real-time PCR. Real-time PCR analysis was performed using TaqMan Universal PCR Master Mix (AB4034437) on an ABI PRISM Sequence Detection System (ABI-SDS) (Applied Biosystems). After reverse transcription, PCR was carried out in triplicate for each mixture, with the synthesized cDNA added to the TaqMan Universal Master Mix and selM AdB product (mixture of sense, antisense, and FAM primer). PCR for glyceraldehyde-3-phosphate dehydrogenase (GAPDH), which served as an endogenous control, was performed simultaneously, with the exception of the rodent GAPDH control reagent (AB4308313). TaqMan probes have two fluorescent dyes; one at the 5'-terminal (Reporter, R), which is used to displace the strand, and the other at the 3'-terminal (Quencher, Q), which is used to block the extension. The reaction mixture was then subjected to amplification with the following sequence profile: 1 cycle of annealing at 50˚C for 2 min, 1 cycle of denaturation at 95˚C for 10 min and 40 cycles of extension at 95˚C for 15 sec and at 60˚C for 2 min. In all cases, an initial denaturation step was carried out at 95˚C for 5 min in order to decrease the formation of a primer-dimer complex under these PCR conditions. The ABI-SDS was programmed to take R and Q fluorescent dye readings after each cycle at a temperature several degrees (60˚C) lower than the melting temperature of the target amplicon. This step was conducted at 60˚C in order to avoid, or at least minimize, any potential contribution to the overall fluorescent dye signals from the primer-dimer formation. A calibration curve was constructed by plotting the R/Q ratio against the amounts of hSelM cDNA synthesized based on the RNA isolated from each tissue of the transgenic rat and from the non-transgenic rat, which were used as the controls.

Western blot analysis. The protein prepared from the tissues of the Tg and non-Tg rat was separated by electrophoresis in a 4-20% SDS-PAGE gel for 3 h and transferred to nitrocellulose membranes for 2 h at 40 V. Each membrane was incubated separately with the primary, anti-SelM (16960; Abcam), and anti-actin (A5316; Sigma) antibodies overnight at 4˚C. The membranes were washed with washing buffer (137 mM NaCl, 2.7 mM KCl, 10 mM Na_2HPO_4, 2 mM KH_2PO_4, and 0.05% Tween-20) and incubated with horseradish peroxidase-conjugated goat anti-rabbit IgG (Zymed) at a 1:1,000 dilution at room temperature for 2 h. The membrane blots were developed using a Chemiluminescence Reagent Plus kit (ECL, Pharmacia).

Immunohistochemistry. Immunohistochemical analysis was performed as previously described (11,12). Briefly, the level

of SelM protein synthesis was determined using optical microscopy after fixing the kidney tissue samples in 5% formalin for 12 h, embedding them in paraffin, and slicing them into 4-μm thick sections. These sections were de-paraffinized with xylene, rehydrated, and pretreated for 30 min at room temperature with a PBS-blocking buffer containing 10% goat serum. The samples were then incubated with the mouse anti-SelM antibody diluted 1:1,000 in PBS-blocking buffer. These antigen-antibody complexes were visualized with the biotinylated secondary antibody goat anti-rabbit-conjugated HRP streptavidin (Histostain-Plus Kit; Zymed) diluted 1:1,500 in a PBS-blocking buffer. The SelM proteins were detected using a stable DAB (ResGen, Invitrogen Corp.) and an Imazing Densitometer (Model GS-690; Bio-Rad).

Analysis of total antioxidant and H_2O_2. The level of total antioxidants and H_2O_2 in the serum and erythrocytes of non-Tg and Tg rats was detected using the *in vitro* quantitative assay procedure and reagents in the Total Antioxidant Status (Randox Labotatories Ltd., Antrim) and Quantitative Hydrogen Peroxide Assay (Oxis International Inc., Portland, OR). For the detection of the total antioxidants, 12 μl of serum and standards was added to 1 ml of chromogen reagent (Metmyoglobin 6.1 μmol, ABTS 610 μmol) in a cuvette. The solutions were mixed well and incubated in order to bring them to room temperature. The cuvettes were then read at 600 nm using a Molecular Devices Vmax Plate reader (Sunnyvale, CA, USA) as the intial absorbance (A_1). The substrates were simultaneously added to the mixture and start timer. After exactly 3 min, the secondary absorbance (A_2) of the cuvettes was read at 600 nm. Finally, the total antioxidant status was calculated using the suggested formula [Total antioxidant status (mmol/l) = Factor x (ΔA blank - ΔA sample), Factor = concentration of standard/(ΔA blank - ΔA standard)].

In order to determine the level of H_2O_2, one volume of sample or standard was added to 10 volumes of working reagent in a cuvette. The two solutions were mixed well and incubated at room temperature for 25-30 min. The spectrophotometer (Ultraspec 1000, Amersham, USA) was prepared on zero status, and the absorbance of the mixture was measured at 560 nm.

Activity analysis of SOD and glutathione peroxidase. The levels of SOD and GPX in erythrocytes from the non-Tg and Tg rats were detected using the calorimetric assay procedure and the reagents in the Bioxytech SOD-525 and Bioxytech GPx-340 kit (OxisResearch™; Portland, OR, USA). The erythrocytes were harvested from the blood by centrifugation at 3,000 rpm for 10 min and were then added to 4 volumes of cold deionized water in order to lyse the cells. This lysate was stored at -70˚C until it was used for the enzyme activity assay. In order to measure the GPX activity, the spectrophotometer was set to measure the absorbance at 340 nm and 23-25˚C. Immediately before the assay, the lysate containing the erythrocytes was diluted with assay buffer, typically 1/10 [for SOD assay: 200 mM manitol, 10 mM Tris-HCl (pH 7.4), 1 mM EDTA, 50 mM sucrose; for the GPX assay: 5 mM EDTA, 50 mM Tris (pH 7.5), 1 mM mercaptoethanol]. In a cuvette, 350 μl of assay buffer, 350 μl of NADPH reagent and 70 μl of the lysate containing erythrocytes were added and mixed well. In addition, 35 μl of working substrate, a 1/10,000 dilution of tert-Butyl hydroperoxide, was added to the cuvette and mixed by pipetting up and down twice. Finally, the absorbance was measured for 3 min in A_{340}. The GPX activity was used to determine the rate of decrease in A_{340} per min. The net rate for GPX activity was calculated by subtracting the rate observed for a water blank from the rate measured for the erythrocyte lysate. The net A_{340} for GPX activity was then converted to the amount of NADPH consumed (nmol/min/ml) using the following relationship: 1 mU/ml = 1 nmol NADPH/min/ml = (A_{340}/min)/0.00622. For SOD activity, 900 μl of reaction buffer (2-amino-2methyl-1,3-propanediol containing boric acid and DTPA, pH, 8.8) was aliquoted into a test tube for each blank or sample. This mixture was then added to 40 μl of sample and 30 μl of R2 reagent (1-methyl-2-vinylpyridinium trifluoromethanesulfonate in HCl) and incubated at 37˚C for 1 min. Finally, 30 μl of R1 reagent (5,6,6a,11b-tetrahydro-3,9,10-trihydroxybenzo[c]fluorine in HCl) was added to the test tube containing the mixture and vortexed briefly. The final mixture was immediately transferred to a spectrophotometric cuvette, and the absorbance was measured by a spectrophotometer at 525±2 nm. The SOD activity was calculated directly from the experimental Vs/Vc ratio using the following equation: [SOD] = 0.93 x (Vs/Vc-1)/1.073 - [0.073 x (Vs/Vc)].

Corticosterone. The enzymeimmunoassay kit used for the quantitative determination of corticosterone in the rat serum was obtained from IDS Inc. (Fountain Hills, AZ, USA). This kit is a competitive enzymeimmunoassay that utilizes a poly-clonal corticosterone antibody that is coated onto the inner surface of polystyrene microtitre wells. All serum samples to be analyzed, including the standard and controls, were assayed in duplicate. In the assay, 100 μl of each calibrator, control and sample were pipetted into the appropriate wells of the antibody-coated plate in duplicate, and 100 μl of enzyme conjugate solution was added. This plate was sealed in a plastic bag and incubated at 2-8˚C for 16-24 h in order to bind corticosterone and their antibodies. After the incubation period, all wells were washed three times with wash solution, and 200 μl of TMB substrate was added using a multichannel pipette. This plate was then incubated at 18-25˚C for 30 min, and 100 μl of stop solution was added to all the wells. Finally, the absorbance of each well was measured at 450 nm using a microplate reader within 30 min of the addition of the stop solution.

Hematological analysis. The blood sample was collected from the abdominal vein of the rat. These collected samples were examined and measured automatically using a hematological autoanalyzer (ADVIA Hematology System, Bayer, NY, USA).

Statistical analysis. The level of SelM protein, GPX activity, SOD activity, total antioxidant concentration, H_2O_2 concentration and coticosterone concentration in the non-Tg and Tg rats were compared using a one-way ANOVA test of variance (SPSS for Windows, release 10.10, standard version, Chicago, IL). In addition, the levels of these factors in the AAPH-treated group and the no-treated group were

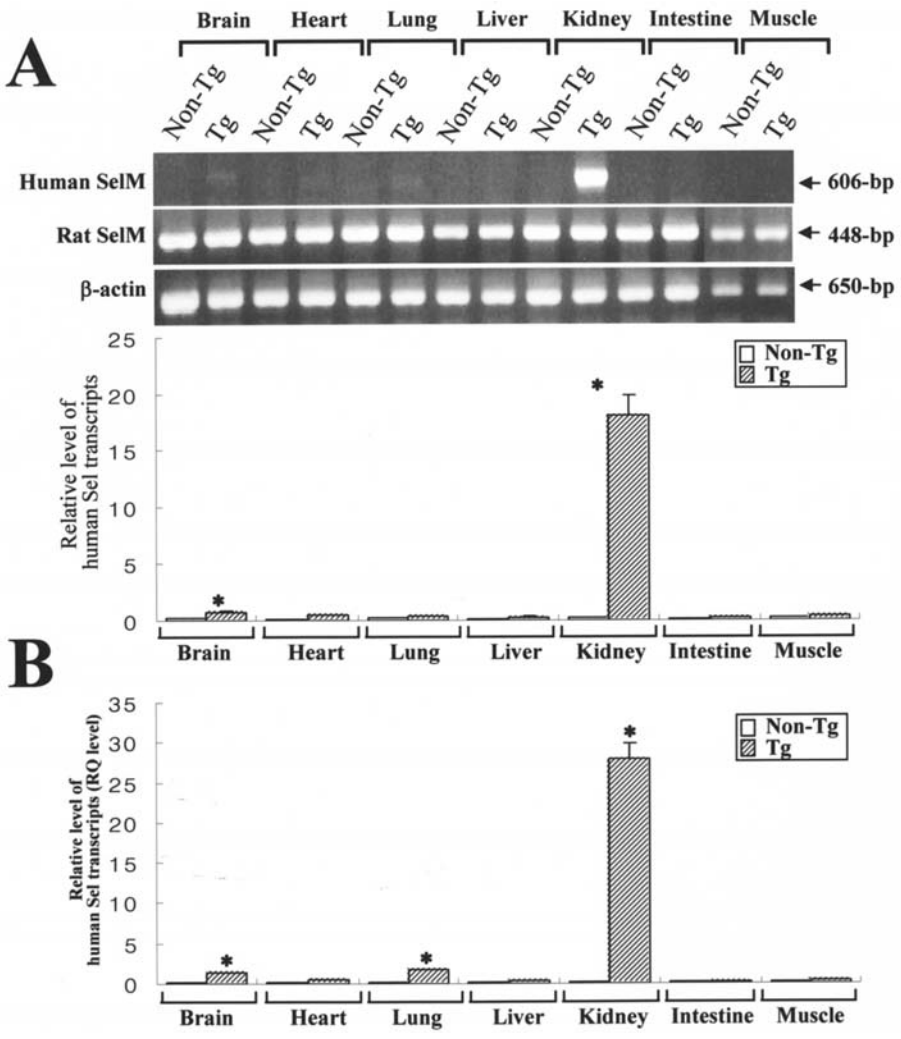

Figure 2. Tissue-specific expression of the human and rat SelM transgenes in the Tg rats. (A) Expression of human and rat SelM in various tissues by RT-PCR. The ß-actin signal was used as the control, and the transcript (650-bp) indicates the RNA loading. In addition, the RT-PCR products for human SelM (606-bp) and rat SelM (448-bp) are indicated. The density of the transcript was quantified using the Kodak Electrophoresis Documentation and Analysis System 120. (B) Real-time PCR analysis of human SelM expression. Calibration was constructed by plotting the R/Q ratio against the amounts of human SelM cDNA synthesized based on the RNA isolated from the tissue of the transgenic rat and from the tissue of the non-transgenic rat used as the control. The data represent the mean ± SEM from three replicates. *p<0.05; significant difference between the Tg and non-Tg rat.

compared using an unpaired t-test. All values were represented as the mean ± standard deviation (SD). A p-value <0.05 was considered significant.

Results

Tg rat production. In order to produce the CMV/EGFP-hSelM Tg rat expressing the hSelM protein in each tissue, the *CMV/EGFP-hSelM* fragment (3,183-bp) was microinjected into the male pronucleus of fertilized embryos that were obtained by crossing a female with a male Wistar-Imamichi rat. Of a total of 28 offspring (11 males and 17 females), 2 females (#68, #81) from the first lineage founder rat possessed the *CMV/EGFP-hSelM* gene, which was identified by genomic DNA-PCR using the hSelM specific primer (Fig. 1B and C). The founder mice containing *CMV/EGFP-hSelM* were then mated with the Wistar-Imamichi rats in order to produce a large number of animals. The *CMV/EGFP-hSelM* gene introduced into their genomes was transmitted to all offspring with ~50% hemizygotes in a Mendelian fashion.

Tissue-specific regulation of hSelM expression in the CMV/GFP-hSelM Tg rat. In order to determine whether the regulation of the introduced *hSelM* gene was expressed under the control of the CMV promoter in all tissues, the transcriptional levels of SelM from various tissues, including the brain, heart, lung, liver, kidney, intestine, and muscles of Tg rats were examined by RT-PCR and real-time PCR analysis. The RT-PCR analysis showed that the highest level of hSelM expression was observed in the kidney, followed by the brain, lung, heart, liver, muscles and intestine (Fig. 2A). However, the expression level of endogenous rat SelM in all of the tissue samples analyzed did not differ between the non-Tg and Tg rats. Furthermore, real-time PCR analysis showed a significantly higher expression level of the hSelM transcripts (RQ level) in the kidney and brain of the CMV/GFP-hSelM Tg rats (Fig. 2B), as indicated by the data from the RT-PCR analysis. Furthermore, total SelM protein expression in the kidney of the Tg rat was examined by Western blotting and immunostaining. As shown in Fig. 3, the GFP-hSelM fusion proteins (52-kDa) were detected by Western blotting using

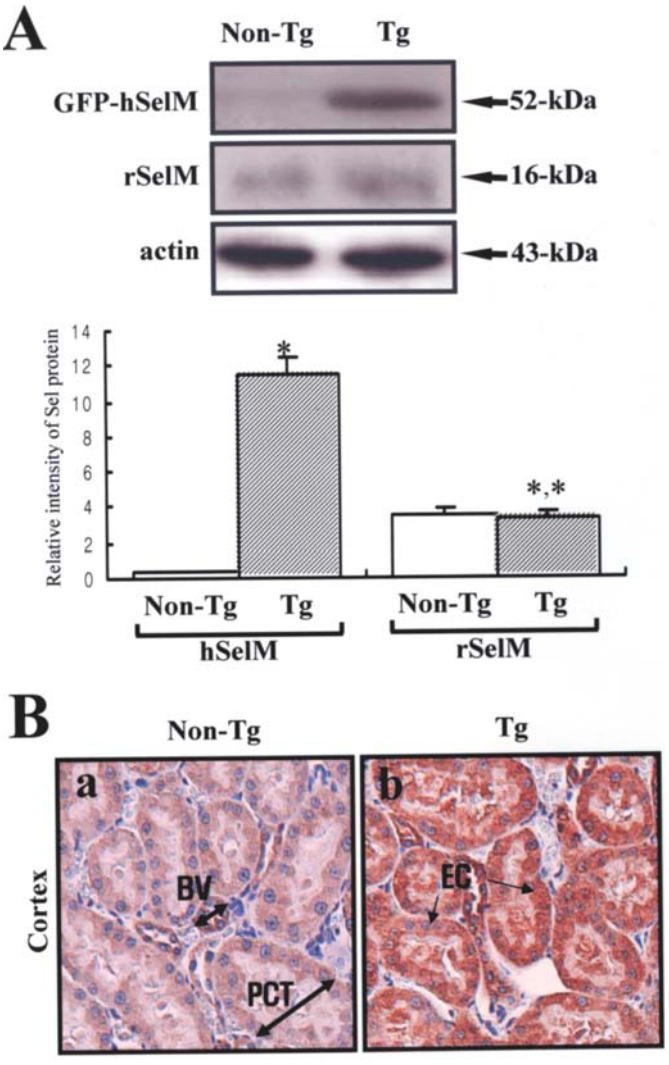

Figure 3. The level of SelM protein expression in the kidney. (A) Expression of the human and rat SelM proteins according to Western blot analysis. The membranes were incubated with antibodies for SelM and the ß-actin protein from the kidney cytosol fraction. These antibodies recognized the SelM originating from rats and humans. Three rats per group were assayed by Western blotting. The values are reported as the mean ± SD; $p<0.05$ vs the control. (B) Immunostaining analysis of SelM expression. The expression profile of SelM in the kidney at 10 weeks of age by immunostaining analysis. A high intensity was observed in the kidney (b) of the CMV/GFP-hSelM Tg rat as compared with the non-Tg rat at x200 magnification. The data represent the mean ± SEM from three replicates. $^{*}p<0.05$; significant difference between Tg and non-tg rats.

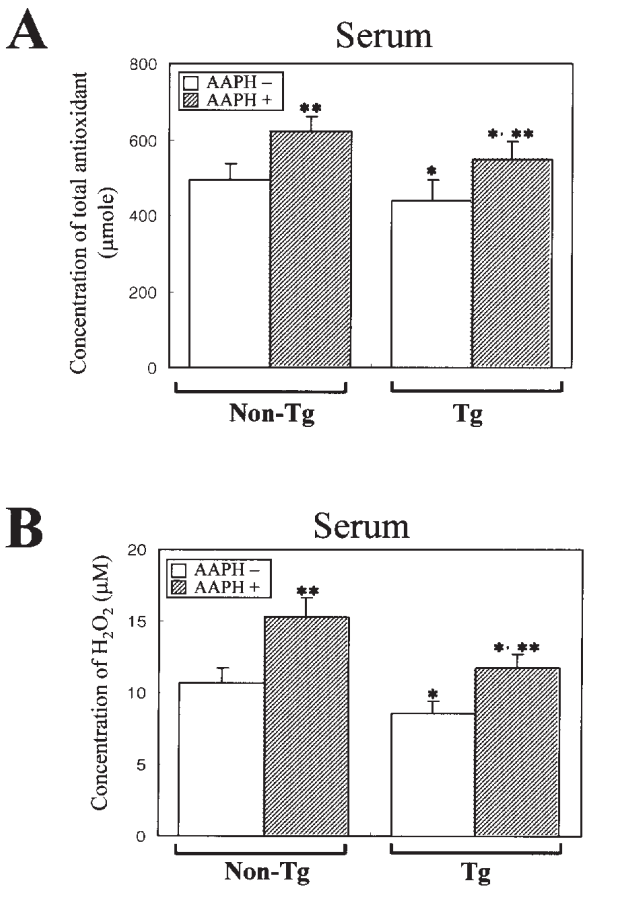

Figure 4. Effect of SelM overexpression on the concentration of total antioxidants and H_2O_2 in the serum. The serum used in this assay was collected from Tg and non-Tg rats after an i.p. injection of AAPH (100 mg/kg BW). Six rats per group were assayed in the ELISA test. The data represent the mean ± SEM from three replicates. $^{*}p<0.05$; significant difference between Tg and non-Tg rats. $^{**}p<0.05$; significant difference between the AAPH-treated group and no-treated group per genotype.

the specific antibody for the rat/human SelM proteins in the kidney tissues of the CMV/GFP-hSelM Tg rat. In particular, the level of GFP-hSelM fusion proteins was significantly higher in the kidney of the Tg rat than in that of the non-Tg rat. In contrast, a low level of the endogenous rat SelM protein was simultaneously detected in both the non-Tg and Tg rats (16-kDa) (Fig. 3A). In order to detect the localization and distribution of the SelM protein in various tissues, SelM protein immunoreactivity was analyzed in the kidney using optical microscopy. The immunostaining intensity in the CMV/GFP-hSelM Tg rat was spread throughout the epithelial cells of the renal tubules in the kidney. However, the level of intensity in the non-transgenic litter-mates was slightly lower than that of the Tg rats (Fig. 3B). Therefore, all of the above observations suggest that the regulatory sequence of the hCMV early promoter could be successfully attributed to the synthesis of the SelM transcripts and protein in the CMV/GFP-hSelM Tg rat.

Changes in SOD and GPX activity in the various tissues of the CMV/GFP-hSelM Tg rat. To examine whether SelM can induce changes in the activity of the antioxidant enzyme, the activity level of SOD and GPX was detected in all tissues of the CMV/GFP-hSelM Tg rat using a detection kit containing a specific substrate. In the case of GPX activity, the highest GPX activity at the basal level was observed in the kidney and liver, followed by the heart, lung, intestine, and brain. This enzyme activity in the hippocampus, lung, liver and intestine was significantly increased in the CMV/GFP-hSelM Tg rat when compared to the non-Tg rat, while the activity of this enzyme was slightly increased in the cortex of the brain in the CMV/GFP-hSelM Tg rat. The highest basal level of SOD activity was observed in the kidney and heart, followed by the liver, lung, heart, brain and intestine. Furthermore, this enzyme activity in the cortex, hippocampus and intestine was significantly increased in the CMV/GFP-hSelM Tg rat when compared to the non-Tg rat, while the enzyme activities in

Effects of SelM overexpression on the activities of GPX and SOD in various tissues.[a]

Tissues	GPX (mU/ml)		SOD (mU/ml)	
	Non-Tg	Tg	Non-Tg	Tg
Brain (cortex)	21.4±1.1	22.1±0.9[b]	1.67±0.1	2.63±1.2[b]
Brain (hippocampus)	13.3±1.0	23.5±1.4[b]	1.67±0.1	2.43±1.1[b]
Heart	344.7±25.2	331.3±23.6	4.06±0.3	1.94±0.2[b]
Lung	265.4±20.3	383.5±27.3[b]	2.34±0.2	2.41±0.2
Liver	653.3±29.4	716.1±31.3[b]	2.91±0.2	2.79±0.2
Kidney	712.0±40.7	690.4±33.5	4.24±0.3	3.48±0.3[b]
Intestine	154.3±09.6	238.7±14.9[b]	1.37±0.1	1.98±0.1[b]

[a]The data represent the mean ± SEM from three replicates. [b]$p<0.05$; significant difference between Tg and non-Tg rats.

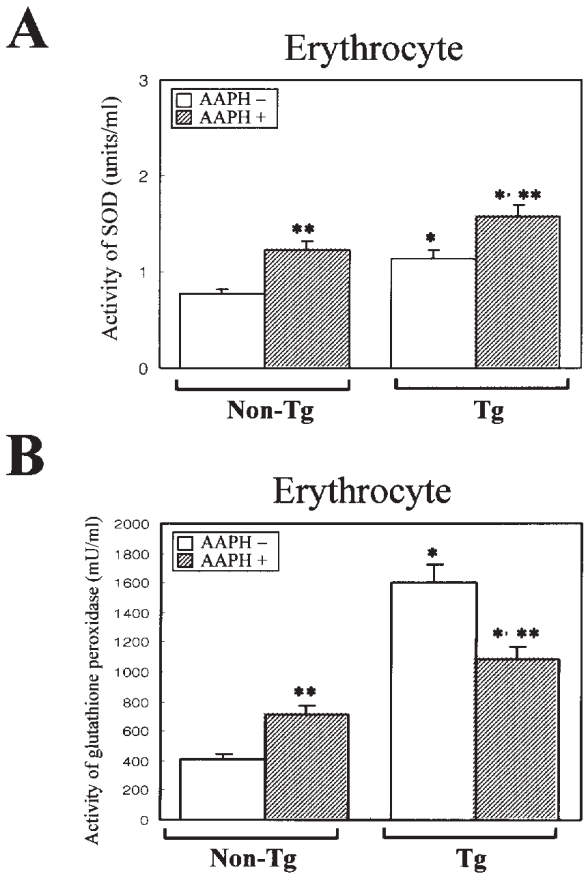

Figure 5. Effect of SelM overexpression on the activity of SOD and GPX in the erythrocytes. The erythrocytes used in this assay were collected from the blood of Tg and non-Tg rats after an i.p. injection of AAPH (100 mg/kg BW). Six rats per group were assayed in the ELISA test. The data represent the mean ± SEM from three replicates. *$p<0.05$; significant difference between Tg and non-Tg rats. **$p<0.05$; significant difference between the AAPH-treated group and no-treated group per genotype.

the heart and kidney were decreased in the CMV/GFP-hSelM Tg rat (Table I). These results suggest that the overexpression of the hSelM protein differentially regulated changes in the activites of GPX and SOD in various tissues of the hSelM-Tg rat.

Effect of SelM overexpression on the H_2O_2 and total antioxidant concentration. The results of earlier studies have established that AAPH leads to the formation of carbon-centered radicals, which yield alklyperoxyl radicals and hydroperoxides that are capable of modifying lipid and DNA under aerobic conditions (13-16). In order to study the effect of hSelM overexpression under high levels of free radicals, the concentration of total antioxidant and H_2O_2 was determined in the serum of CMV/GFP-hSelM Tg and non-Tg rats after AAPH injection using an ELISA kit. For the antioxidant assay, the concentration of total antioxidants at the basal level was significantly lower in the CMV/GFP-hSelM Tg rats than in the non-Tg rats. These levels were significantly increased in both the CMV/GFP-hSelM Tg rat and non-Tg rat after AAPH treatment. However, the concentration of total antioxidants in the CMV/GFP-hSelM Tg rat was consistently maintained at a low level in comparison to the non-Tg rat. In particular, the rate of increase between the no-treated group and the AAPH-treated group was very similar in both the CMV/GFP-hSelM Tg and non-Tg rats (Fig. 4A). In addition, the results obtained from the H_2O_2 assay showed that the increasing pattern of H_2O_2 concentration in the Tg rat was very similar to the results from the total antioxidant assay, after AAPH treatment (Fig. 4B). These results suggest that SelM overexpressed under the control CMV promoter can contribute to the increase in the functional activity for antioxidant protection in the CMV/GFP-hSelM rat.

Changes in SOD and GPX activity in the erythrocytes of CMV/GFP-hSelM Tg rats. In order to determine the cause of the decrease in the total antioxidant and H_2O_2 concentrations in the serum, the activity levels of SOD and GPX were determined in the erythrocytes of CMV/GFP-hSelM Tg rats using a detection kit containing a specific substrate (Fig. 5). The CMV/GFP-hSelM Tg rat showed a slightly higher rate of SOD activity than the non-Tg rat at the basal level, and these patterns were maintained even in the AAPH-treated group. In addition, the GPX activity was significantly increased in the erythrocytes of the CMV/GFP-hSelM Tg rats as compared to non-Tg rats, with a 3- to 4-fold increase. However, in the AAPH-treated group of CMV/GFP-hSelM Tg rats, the GPX activity was preferably decreased in

A

Class	Non-Tg rat		Tg rat	
	AAPH –	AAPH +	AAPH –	AAPH +
Neut	8.9±0.7	48.0±3.5*	9.1±0.9	76.2±6.5*, **
Lymph	87.1±7.3	37.9±3.1*	85.8±7.8	16.8±0.1 *, **
Mono	1.7±0.1	11.2±0.9*	1.7±0.1	4.9±0.4*, **
Eos	0.4±0.03	0.2±0.01*	0.5±0.04	0.5±0.05**
Baso	1.0±0.1	1.6±0.1*	0.9±0.07	0.8±0.07**
Luc	0.9±0.08	1.0±0.1	2.1±0.2	0.7±0.06*,**

B

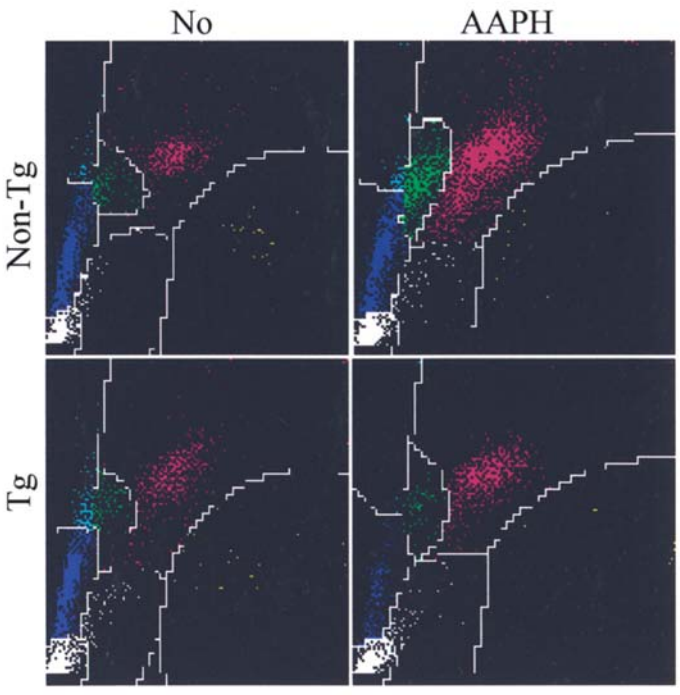

Figure 6. Effect of SelM overexpression on the composition of white blood cells in the hematological value. (A) The composition of the white blood cells. (B) Cytogram of the white blood cells. The blood used in this analysis was collected from Tg and non-Tg rats after an i.p. injection of AAPH (100 mg/kg BW). Six rats per group were assayed in the hematology test. The data represent the mean ± SEM from three replicates. *$p<0.05$; significant difference between Tg and non-Tg rats. **$p<0.05$; significant difference between the AAPH-treated group and the no-treated group per genotype.

comparison to the no-treated group, but these rats maintained a higher level of activity than that in the AAPH-treated group of non-Tg rats. Therefore, these observations suggested that the increase in SOD and GPX activity in the erythrocytes of CMV/GFP-hSelM Tg rats may contribute to the decrease in the total antioxidant and H_2O_2 concentrations in the serum.

Changes in white blood cell (WBC) composition in the transgenic rat. It was reported that selenoprotein and selenium are tightly associated with the progression of infectious diseases (4) and immune cell composition (17). To assay the effects of SelM overexpression on the immune-related cell population, the hematological values were assayed in the blood of both CMV/GFP-hSelM Tg and non-Tg rats after the injection of AAPH. In the no-treated group, the WBC composition among the hematological values did not differ between the CMV/GFP-hSelM Tg rat and the non-Tg rat. However, after AAPH treatment, the number of neutrophils was significantly increased in the CMV/GFP-hSelM Tg rat compared to the non-Tg rat, while the number of lymphocytes, monocytes and basophils was significantly decreased in the Tg rat (Fig. 6). These results were then used to calculate the neutrophil-to-lymphocyte (N/L) ratio. In the no-treated group, the N/L ratio did not differ between the CMV/GFP-hSelM Tg and non-Tg rats. However, the N/L ratio in the AAPH-treated group was two to three times higher in the CMV/GFP-hSelM Tg rats than in the non-Tg rats (Fig. 7A). Therefore, these results suggest that hSelM protein overexpression can induce a composition change in immune-related cells in response to AAPH agents.

Changes in corticosterone in the transgenic rat. Numerous studies have reported that the increased level of corticosterone causes an increase in the N/L ratio by destructing

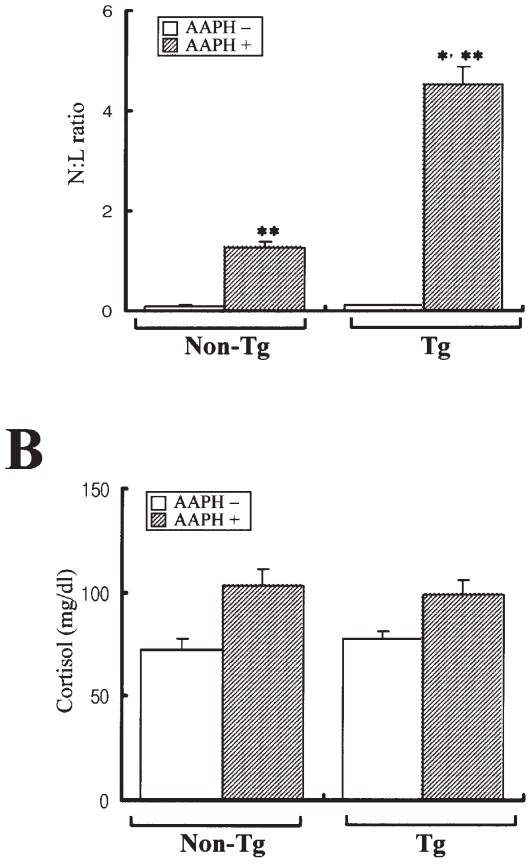

Figure 7. Effect of SelM overexpression on the N/L ratio and concentration of corticosterone. (A) Change in the N/L ratio of the AAPH-treated Tg rat. (B) Change in the serum corticosterone level. The serum was collected from the blood of the abdominal veins of the Tg and non-Tg rats after AAPH treatment. Six rats per group were assayed in the ELISA test. The data represent the mean ± SEM from three replicates. $^{*}p<0.05$; significant difference between Tg and non-Tg rats. $^{**}p<0.05$; significant difference between the AAPH-treated group and the no-treated group per genotype.

the lymphocytes in the thymus cortex or by extending the neutrophil half-life (18,19). Therefore, to study the correlation between the N/L ratio and corticosterone concentration, the concentration of corticosterone was assayed in the serum from CMV/GFP-hSelM Tg and non-Tg rats using an ELISA kit to coat the specific antibody. The concentration of corticosterone in the AAPH-treated group was significantly increased when compared to the no-treated group in both CMV/GFP-hSelM Tg and non-Tg rats. However, the increased rate and patterns of corticosterone concentration in the CMV/GFP-hSelM Tg and non-Tg rats showed no differences (Fig. 7B). These results suggest that corticosterone may not contribute to the composition change of immune-related cells in the Tg rat overexpressing the hSelM protein in response to the AAPH chemical.

Discussion

Selenium is an essential trace element for animal and human health that is obtained through the diet (20,21). Deficiencies in this element are associated with a predisposition to certain conditions, including cancer, atherosclerosis, arthritis, male infertility, immunological defects and accelerated aging (22,23). In addition, selenium is thought to exert its biological function primarily through selenoproteins, which contain selenium in their active centers as a part of the 21st natural amino acid selenocystein (8,24,25).

Selenocystein is synthesized cotranslationally from serine and selenide as selenocysteine by a series of enzymatic reactions dictated by the UGA codon (26) and SECIS sequences (27,28). Synthesized selenocystein is incorporated into at least 24 or 25 different gene products, selenoproteins, in humans and rodents, respectively (25). This protein family performs a wide spectrum of biological functions, ranging from antioxidant protection and thyroid hormone metabolism to proper reproductive performance (22). Moreover, selenoproteins are crucial to many cellular functions as demonstrated by the fact that the overexpression of glutathione peroxidase 1 (29,30) and thioredoxin reductase (31) has been found to inhibit apoptosis as well as the finding that selenoprotein P seems to be a survival factor for neurons (32,33).

No homologous protein to SelM was found in a non-reduced database when analyzed by default BLAST programs. However, the use of advanced sequence analysis tools revealed a distant homology to the 15-kDa selenoprotein (Sel15). Moreover, the location of Sec was conserved between these two proteins. However, Sep15 had a Cys-Gly-Sec-Lys motif, whereas SelM contained Sec in a Cys-Gly-Gly-Sec motif. This motif sequence was similar to the sequences found in the eukaryotic selenoproteins SelW and SelT (7).

The expression system containing the hSelM cDNA under the control of the CMV promoter was successfully expressed in several tissues of the CMV/GFP-hSelM Tg rat at the RNA level. In particular, the highest level of hSelM expression was observed in the kidney, followed by the brain, lung, heart, liver, muscles and intestine. Western blotting and immunostaining showed that there was also a significantly higher level of the human SelM protein in the kidney of the CMV/GFP-hSelM Tg rat than in the non-Tg rat, which was used as the control. Therefore, this expression system expressing the GFP-hSelM fusion gene was successfully introduced into the genomic DNA of the CMV/GFP-hSelM Tg rat, which expressed the RNA and protein required to induce the activation of antioxidant protection in the CMV/GFP-hSelM Tg rat for the first time.

GPX1 is the first identified (34) and most abundant selenoprotein in mammals (35,36). This enzyme is expressed in both the cytosol and mitochondria (37) and uses glutathione to reduce H_2O_2 and organic hydroperoxides. In the previous study, the overexpression of the GPX1 gene in mice demonstrated that the GPX1 activities in the liver and soleus muscles of Tg rats were 21% and 3 times greater than that of wild-type mice, respectively. However, the activity of other selenium-dependent or antioxidant enzymes, including GPX3, GPX4, thioredoxin reductase, glutathione S-transferase, CuZn-superoxide dismutase, and Mn-superoxide dismutase in the plasma, liver, or muscle was very similar between the CMV/GFP-hSelM Tg and non-Tg rats (38). In this study, to investigate the effects of SelM overexpression on the activity of the antioxidant enzyme, the activities of

GPX and SOD were detected in the various tissues of Tg rats. The GPX activity was significantly increased in the brain, lung, liver, and intestine, but did not change in the heart and kidney. In addition, the activity of SOD was increased only in the brain hippocampus and intestine, but decreased in the brain cortex, heart and kidney. Therefore, these results suggest that the overexpression of the SelM protein in various tissues may differentially regulate the activity of two antioxidant enzymes.

AAPH agents are widely used as an initiator to free radical generation in the animal body. Terao and Niki (39) found that the intraperitoneal injection of AAPH induced mitochondrial swelling and macrovesicular fatty degeneration of hepatocytes without hepatocyte necrosis *in vivo*. Furthermore, the AAPH-dependent formation of alkyl-hydroperoxide increased linearly with time and led to a 40% inactivation of GPX in 1 h to complete inactivation in 4 h (40). In this study, we examined whether the overexpression of the SelM protein in a Tg rat could change the concentration of total antioxidants and H_2O_2 in response to AAPH. In serum, the free radical generated by AAPH significantly increased the concentration of total antioxidants and H_2O_2 in the AAPH-treated group when compared to the no-treated group of non-Tg rats. Furthermore, the CMV/GFP-hSelM Tg rat overexpressing hSelM showed lower antioxidant and H_2O_2 concentrations than the non-Tg rat, even though the increased pattern of antioxidant and H_2O_2 concentration by AAPH treatment was very similar between the CMV/GFP-hSelM Tg and non-Tg rats. In particular, we observed the activity levels of key enzymes for the antioxidant process, including SOD and GPX, in the erythrocytes of Tg rats in order to search for a direct cause of the decrease in the concentrations of antioxidants and H_2O_2. The activities of these two enzymes were significantly higher in the erythrocytes of the CMV/GFP-hSelM Tg rat than in those of the non-Tg rat. The activities of these enzymes were increased in both rats after AAPH treatment, but no increases in the activity of the GPX enzyme were observed in the CMV/GFP-hSelM Tg rat. These results suggest that SelM overexpression in the CMV/GFP-hSelM Tg rat may have contributed to the decrease in the concentration of antioxidants and H_2O_2 by upregulating the two antioxidant enzymes.

Several infectious diseases were essentially associated with the oxidative stress exerted by the innate immune response of the host. This self-protecting cellular system of the host comprised SOD and, of the selenoproteins, GPX, and possibly selenoprotein P (4). However, the relationship between the selenium status of the host and bacterial infection has not been well investigated, although the hypothesis predicting the aggravation of disease by selenium deficiency due to impaired antioxidant defense equally applies (4). Jaeschke *et al* (41) reported that the application of bacterial lipopoly-saccharide induced the death of GPX (-/-) mice more readily than wild-type mice, and the increased susceptibility of knock-out mice could not be modified by titrating down and up the remaining selenoproteins by selenium deprivation/resupplementation. This study examined the effects of SelM overexpression on the composition of immune-related cells. The number of neutrophils in the AAPH-treated group was significantly increased in the CMV/GFP-hSelM Tg rat when compared to the non-Tg rat, while the number of lymphocytes decreased by 5-fold. As a result, the N/L ratio was three times higher in the CMV/GFP-hSelM Tg rat than in the non-Tg rat.

Finally, to verify that SelM overexpression in the CMV/GFP-hSelM Tg rat can act as the major factor responsible for changing the N/L ratio, the concentration of corticosterone was detected in the serum of Tg rats using an ELISA kit-coated specific antibody as corticosterone is known to play the role of a key hormone regulating the N/L ratio by destructing lymphocytes or extending the half-life of neutrophils (18). In this study, no differences were observed in the concentration of corticosterone between the CMV/GFP-hSelM Tg and non-Tg rats without regard to AAPH treatment. Therefore, these results showed that SelM overexpression rather than the corticosterone level may contribute to the increased N/L ratio in the blood of Tg rats in response to AAPH injection. In addition, this CMV/GFP-hSelM Tg rat containing a large number of neutrophils has the potential to provide rapid defense against bacterial infections and other very small inflammatory processes.

All of the aforementioned results showed that the CMV/GFP-hSelM Tg rat can serve as an animal model for the maintenance of a high level of antioxidant status in order to study infectious diseases, neurodegenerative disorders, cardiovascular disease and cancer. However, in order to investigate these diseases, the physiological characteristics of the CMV/GFP-hSelM Tg rat need to be determined because these Tg rats may be used to examine the entire SelM-related metabolism in comparison with other selenoprotein-related animal models.

Acknowledgements

The authors wish to acknowledge the animal technicians Sunmi Choi, B.S. and Ms. Jermlan Song for directing the Animal Facility and Care at the Division of Laboratory Animal Resources. This research was supported by a grant from the Scientific Research division of the Korea FDA.

References

1. Kryukov GV, Castellano S, Novoselov SV, Lobanov AV, Zehtab O, Guigo R and Gladyshev VN: Characterization of mammalian selenoproteomes. Science 300: 1439-1443, 2003.
2. Kyriakopoulos A and Behne D: Selenium-containing proteins in mammals and other forms of life. Rev Physiol Biochem Pharmacol 145: 1-46, 2002.
3. Schweizer U, Brauer AU, Kohrle J, Nitsch R and Savaskan NE: Selenium and brain function: a poorly recognized liaison. Brain Res Rev 45: 164-178, 2004.
4. Birringer M, Pilawa S and Flohe L: Trends in selenium biochemistry. Nat Prod Rep 19: 693-718, 2002.
5. Savaskan NE, Alvarez-Bolado G, Glumm R, Nitsch R, Skutella T and Heimrich B: Impaired postnatal development of hippocampal neurons and axon projections in the $Emx2^{-/-}$ mutants. J Neurochem 83: 1196-1207, 2002.
6. Diwadkar-Navsariwala V, Prins GS, Swanson SM, Birch LA, Ray VH, Hedayat S, Lantvit DL and Diamond AM: Selenoprotein deficiency accelerates prostate carcinogenesis in a transgenic model. Proc Natl Acad Sci USA 103: 8179-8184, 2006.
7. Korotkov KV, Novoselov SV, Hatfield DL and Gladyshev VN: Mammalian selenoprotein in which selenocysteine (Sec) incorporation is supported by a new form of Sec insertion sequence element. Mol Cell Biol 22: 1402-1411, 2002.

ov GV, Schmidt S and Sunyaev S: Small fitness effect of ons in highly conserved non-coding regions. Hum Mol Genet 14: 2221-2229, 2005.
9. Muller WE, Borejko A, Brandt D, Osinga R, Ushijima H, Hamer B, Krasko A, Xupeng C, Muller IM and Schroder HC: Selenium affects biosilica formation in the demosponge *Suberites domuncula*. Effect on gene expression and spicule formation. FEBS J 272: 3838-3852, 2005.
10. Hwang DY, Cho JS, Oh JH, Shim SB, Jee SW, Lee SH, Seo SJ, Lee SK, Lee SH and Kim YK: Differentially expressed genes in transgenic mice carrying human mutant presenilin-2 (N141I): correlation of selenoprotein M with Alzheimer's disease. Neurochem Res 30: 1009-1019, 2005.
11. Hwang DY, Chae KR, Kang TS, Hwang JH, Lim CH, Kang HK, Goo JS, Lee MR, Lim HJ, Min SH, Cho JY, Hong JT, Song CW, Paik SG, Cho JS and Kim YK: Alterations in behavior, amyloid beta-42, caspase-3, and Cox-2 in mutant PS2 transgenic mouse model of Alzheimer's disease. FASEB J 16: 805-813, 2002.
12. Hwang DY, Seo SJ, Kim YK, Kim CK, Shim SB, Jee SW, Lee SH, Sin JS, Cho JY, Kang BC, Jang IS and Cho JS: Significant change in insulin production, glucose tolerance and ER stress signaling in transgenic mice coexpressing insulin-siRNA and human IDE. Int J Mol Med 19: 65-73, 2007.
13. Hiramoto K, Jojkoh H, Sako K and Kikugawa K: DNA breaking activity of the carbon-centered radical generated from 2,2'-azobis(2-amidinopropane) hydrochloride (AAPH). Free Radic Res Commun 19: 323-332, 1993.
14. Lazar M, Rychly J, Klimo V, Pelikan P and Valko L: Free Radical in Chemistry and Biology. CRC Pree, Boca Raton, FL, pp10-16, 1989.
15. Ma Y-S, Stone WL and LeClair IO: The effects of vitamin C and urate on the oxidation kinetics of human low-density lipoprotein. Proc Soc Exp Biol Med 2: 53-59, 1994.
16. Landi L, Fiorentini D, Galli MC, Segura-Auguilar J and Beyer RE: DT-Diaphorase maintains the reduced state of ubiquinones in lipid vesicles thereby promoting their anti-oxidant function. Free Radic Biol Med 22: 329-335, 1997.
17. Tapiero H, Townsend DM and Tew KD: The antioxidant role of selenium and seleno-compound. Biomed Pharmacother 57: 134-144, 2003.
18. Davies KJ, Delsignore ME and Lin SW: Protein damage and degradation by oxygen radicals. II. Modification of amino acids. J Biol Chem 262: 9902-9907, 1987.
19. Kim CY, Han JS, Suzuki T and Han SS: Indirect indicator of transport stress in hematological values in newly acquired cynomolgus monkeys. J Med Primatol 34: 183-192, 2005.
20. Burk RF: Selenium, an antioxidant nutrient. Nutr Clin Care 5: 75-79, 2002.
21. Neve J: Selenium as a 'nutraceutical': how to conciliate physiological and supra-nutritional effects for an essential trace element. Curr Opin Clin Nutr Metab Care 5: 659-663, 2002.
22. Rayman MP: The importance of selenium to human health. Lancet 356: 233-241, 2000.
23. Brown KM and Arthur JR: Selenium, selenoproteins and human health: a review. Public Health Nutr 4: 593-599, 2001.
24. Atkins JF and Gesteland RF: The twenty-first amino acid. Nature 407: 463-465, 2000.
25. Kryukov GV, Kryukov VM and Gladyshev VN: New mammalian selenocysteine-containing proteins identified with an algorithm that searches for selenocysteine insertion sequence elements. J Biol Chem 274: 33888-33897, 2003.
26. Leinfelder W, Zehelein E, Mandrand-Berthelot MA and Bock A: Gene for a novel tRNA species that accepts L-serine and cotranslationally inserts selenocysteine. Nature 331: 723-725, 1988.
27. Sunde RA: Molecular biology of selenoproteins. Annu Rev Nutr 10: 451-474, 1990.
28. Stadtman TC: Selenocysteine. Annu Rev Biochem 65: 83-100, 1996.
29. Lu YP, Lou YR, Yen P, Newmark HL, Mirochnitchenko OI, Inouye M and Huang MT: Enhanced skin carcinogenesis in transgenic mice with high expression of glutathione peroxidase or both glutathione peroxidase and superoxide dismutase. Cancer Res 57: 1468-1474, 1997.
30. Esworthy RS, Baker MA and Chu FF: Expression of selenium-dependent glutathione peroxidase in human breast tumor cell lines. Cancer Res 55: 957-962, 1995.
31. Gladyshev VN, Factor VM, Housseau F and Hatfield DL: Contrasting patterns of regulation of the antioxidant selenoproteins, thioredoxin reductase, and glutathione peroxidase, in cancer cells. Biochem Biophys Res Commun 251: 488-493, 1998.
32. Yan J and Barrett JN: Purification from bovine serum of a survival-promoting factor for cultured central neurons and its identification as selenoprotein-P. J Neurosci 18: 8682-8691, 1998.
33. Mostert V: Selenoprotein P: properties, functions, and regulation. Arch Biochem Biophys 376: 433-438, 2000.
34. Rotruck JT, Pope AL, Ganther HE, Swanson AB, Hafeman DG and Hoekstra WG: Selenium: biochemical role as a component of glutathione peroxidase. Science 179: 588-590, 1973.
35. Cheng WH, Ho YS, Ross DA, Valentine BA, Combs GF and Lei XG: Cellular glutathione peroxidase knockout mice express normal levels of selenium-dependent plasma and phospholipid hydroperoxide glutathione peroxidases in various tissues. J Nutr 127: 1445-1450, 1997.
36. Cheng WH, Ho YS, Ross DA, Han Y, Combs GF Jr and Lei XG: Overexpression of cellular glutathione peroxidase does not affect expression of plasma glutathione peroxidase or phospholipid hydroperoxide glutathione peroxidase in mice offered diets adequate or deficient in selenium. J Nutr 127: 675-680, 1997.
37. Esposito LA, Kokoszka JE, Waymire KG, Cottrell B, MacGregor GR and Wallace DC: Mitochondrial oxidative stress in mice lacking the glutathione peroxidase-1 gene. Free Radic Biol Med 28: 754-766, 2000.
38. McClung JP, Roneker CA, Mu W, Lisk DJ, Langlais P, Liu F and Lei XG: Development of insulin resistance and obesity in mice overexpressing cellular glutathione peroxidase. Proc Natl Acad Sci USA 101: 8852-8857, 2004.
39. Terao K and Niki E: Damage to biological tissues induced by radical initiator 2,2'-azobis(s-amidinopropane) dihydrochloride and its inhibition by chain-breaking antioxidants. Free Radic Biol Med 2: 193-201, 1988.
40. Ma YS, Chao CC and Stadtman ER: Oxidative modification of glutamine synthetase by 2,2'-azobis(2-amidinopropane) dihydrochloride. Arch Biochem Biophys 363: 129-134, 1999.
41. Jaeschke H, Ho YS, Fisher MA, Lawson JA and Farhood A: Glutathione peroxidase-deficient mice are more susceptible to neutrophil-mediated hepatic parenchymal cell injury during endotoxemia: importance of an intracellular oxidant stress. Hepatology 29: 443-450, 1999.